# ATTRACTIVE LEVITATION FOR HIGH-SPEED GROUND TRANSPORT WITH LARGE GUIDEWAY CLEARANCE AND ALTERNATING-GRADIENT STABILIZATION

John R. Hull
Argonne National Laboratory, Argonne, IL 60439 USA

This paper describes an attractive levitation concept that results in large guideway clearance and low magnetic drag, and requires no feedback for stability. Dynamic stability is achieved by establishing alternating gradients of force, in which the spatial dependence of the attractive force between superconducting coils on the vehicle and iron rails in the guideway is altered by periodic changes in the rail configuration. For a vehicular velocity of 500 km/h, the appropriate lengths for each configuration are in the range of 5 to 40 m, and the guideway clearance is in the range of 50 to 100 mm, depending on the details of the rail and vehicle magnet design.

## Introduction

The use of magnetic levitation for high-speed ground transport (HSGT) has focused mainly on two general methods: (1) electromagnetic suspension (EMS), in which the attractive force between an electromagnet and an iron rail is used to levitate the vehicle; and (2) electrodynamic suspension (EDS), in which the eddy currents induced by the passage of a magnet over a conducting guideway provide a repulsive levitational force. The EMS method is characterized by low magnetic drag, but it results in a small guideway clearance owing to the relatively low field strength of the electromagnet; in addition, it requires active feedback for stability. The EDS method employs the high magnetic field strengths of superconducting magnets to achieve large guideway clearance and is self-stabilizing without feedback, but it results in substantial magnetic drag. Other levitation methods that are potentially useful for HSGT, but have yet to reach the experimental prototype stage, include null-flux suspension [1,2] and mixed-mu suspension [3].

This paper describes an attractive-levitation method that results in large guideway clearance and low magnetic drag and requires no feedback for stability, a combination that could result in substantial cost savings in a HSGT system relative to systems that are based on EDS or EMS. Depending on acceleration requirements, lower magnetic drag can result in lower capital cost for the propulsion system. Larger gap clearance usually implies that guideway tolerances can be relaxed, which usually results in the possibility of a lighter weight and lower cost guideway.

## Alternating-Gradient Attractive Levitation

The method presented here is analogous to that used in strong-focusing synchrotron particle accelerators [4-6] and is based on establishing alternating gradients of force to achieve stability. The spatial dependence of the attractive force between superconducting coils on the vehicle and iron rails in the guideway is altered by periodic changes in the rail configuration. The large magnetic field strengths associated with the superconducting magnets result in a large levitation force, even at guideway clearances approaching those typical of EDS systems. The use of alternating-gradient stabilization in devices using attractive magnetic levitation was first suggested by Hull [7].

A cross section of an example implementation of the concept is shown in Fig. 1, where two current-carrying conductors of a vehicle coil are suspended below a pair of iron rails. The origin of the coordinate system corresponds to the center point of the vehicle coil; coordinate z denotes the vertical separation of the plane of the coil from the plane of the rail pair; and coordinate x denotes the horizontal displacement of the coil centerline from the rail pair centerline. At equilibrium, where the force of gravity is exactly balanced by the vertical magnetic force, the coil is horizontally centered below the pair of rails.

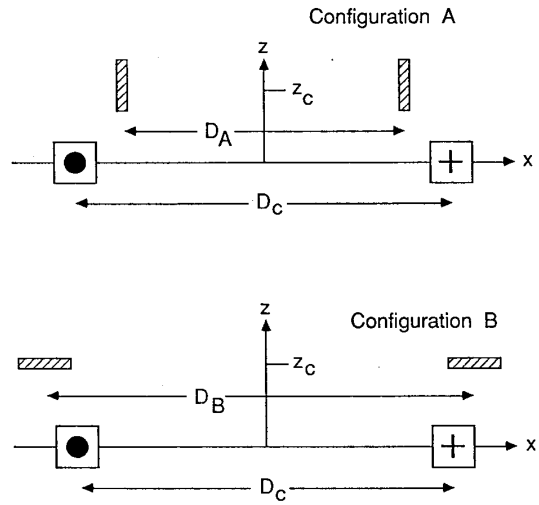


Fig. 1. Coordinate system for the basic geometry of alternating-gradient attractive levitation.

A plot of the vertical magnetic attractive force $F_z$ as a function of the vertical separation z between the coil and the track at x = 0 is shown in Fig. 2 for the two configurations. The equilibrium value in this example is 19.5 kN/m. The corresponding sideways horizontal force $F_x$ as a function of horizontal coordinate x is shown in Fig. 3 for equilibrium values of z. At equilibrium, the system is statically unstable, as expected from Earnshaw's theorem [8]. In Configuration A, the system is stable in the z direction, but unstable in the x direction. In Configuration B, the system is stable in the x direction, but unstable in the z direction. There are two possible equilibrium values of z for Configuration A, but only the lowest value is used. At the larger equilibrium value, the system is unstable in the z direction.

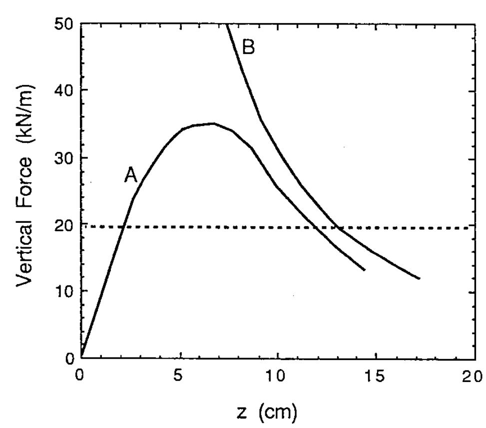


Fig. 2. Vertical magnetic attractive force as a function of vertical coordinate $z_c$ of coil center, for x = 0. The vertical force at equilibrium is 19.5 kN/m and is indicated by the dashed line.

0018-9464/89/0900-3272$01.00©1989 IEEE

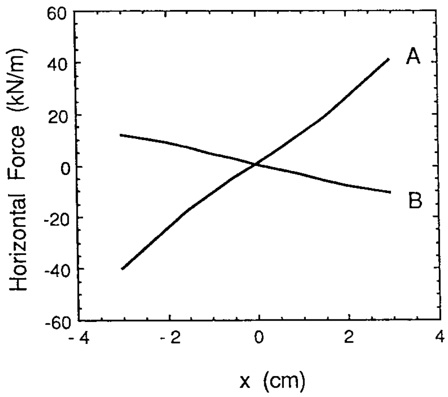


Fig. 3. Horizontal force as a function of horizontal coordinate x at equilibrium points in the vertical direction, $z = z_A$ and $z = z_B$.

With the method of alternating gradients, the system is dynamically stable as the vehicle coil moves in the y direction (in or out of the page in Fig. 1) within some velocity range. At regular points along the vehicular trajectory, the rail configuration switches alternately between A and B. When the vehicle is in the correct velocity range, it is dynamically stable in both directions.

Ignoring damping of motion and rotation about the y-axis, the equations of motion for the coil may be written as follows:

$$d^2z/dt^2 = -\alpha_1 g z, \qquad \text{Configuration A,} \tag{1}$$

$$d^2x/dt^2 = \beta_1 g x, \qquad \text{Configuration A,} \tag{2}$$

$$d^2z/dt^2 = \alpha_2 g z, \qquad \text{Configuration B,} \tag{3}$$

$$d^2x/dt^2 = -\beta_2 g x, \qquad \text{Configuration B,} \tag{4}$$

where g is the acceleration of gravity, and $\alpha$ and $\beta$ are positive coefficients that are approximated here as constants. Letting v denote the vehicular velocity in the y direction, and $L_1$ and $L_2$ the respective lengths of Configurations A and B, we define

$$Z_{11} = \cosh K_2 \cos K_1 + \frac{V_2{}^2 - V_1{}^2}{2V_2V_1} \sinh K_2 \sin K_1 \tag{5}$$

$$X_{11} = \cosh M_1 \cos M_2 + \frac{W_1{}^2 - W_2{}^2}{2W_2W_1} \sinh M_1 \sin M_2 \tag{6}$$

where

$$K_1 = L_1(\alpha_1 g)^{1/2}/v, \qquad V_1 = K_1/L_1,$$

$$K_2 = L_2(\alpha_2 g)^{1/2}/v, \qquad V_2 = K_2/L_2,$$

$$M_1 = L_1(\beta_1 g)^{1/2}/v, \qquad W_1 = M_1/L_1,$$

$$M_2 = L_2(\beta_2 g)^{1/2}/v, \qquad W_2 = M_2/L_2.$$

The system is dynamically stable when

$$-1 \le Z_{11} \le 1, \text{ and} \tag{7}$$

$$-1 \le X_{11} \le 1. \tag{8}$$

To implement the alternating-gradient method in a HSGT system, the desired vehicular velocity would be specified at each point along the route. Guideway geometry and configuration lengths would be chosen to correspond to the velocity profile, and provide for maximum stability at each point of the route. In principle, by choosing very small configuration lengths, levitation could be stable at all but the lowest velocities. Because stability is maintained over a range of velocities for each configuration, typical variations from the design velocity could be tolerated. Extreme deviations from the design velocity, such as those occurring during emergency stops, would require additional stabilization, perhaps by auxiliary electromagnets with active feedback. Changes in vehicular load can be readily accommodated by adjusting the current in the superconducting magnet. To a first approximation, the forces shown in Figs. 2 and 3 scale with the current, whereas the shape of the curves changes little.

## Calculational Examples

As a calculational example, we examine the simple two-dimensional system depicted in Fig. 1, where the cross sections are 50 mm by 50 mm for each conductor, 20 mm by 75 mm for each rail in Configuration A, and 80 mm by 15 mm for each rail in Configuration B. The conductor has a current density of 200 A/mm$^2$, and the rail has a BH curve typical of low-carbon steel. The magnetic fields and forces are calculated numerically as a function of x and z with the static field solver of the computer code PE2D [9], assuming $D_C = 2.15$ m, $D_A = 1.98$ m, and $D_B = 2.21$ m. The corresponding equilibrium values for z are $z_A = 22$ mm, and $z_B = 133$ mm. The curves in Figs. 2 and 3 are examples of the calculational results. The corresponding gradient coefficients at equilibrium are $\alpha_1 = 42.2$ m$^{-1}$, $\alpha_2 = 13.4$ m$^{-1}$, $\beta_1 = 58.2$ m$^{-1}$, $\beta_2 = 10.0$ m$^{-1}$. At equilibrium, the minimum track clearance is 50 mm and occurs in Configuration A.

We assume a vehicular velocity v = 139 m/s (500 km/h). To determine the appropriate guideway segment lengths for each configuration, we plot $X_{11} = 1$, $X_{11} = -1$, $Z_{11} = 1$, and $Z_{11} = -1$ in the $L_A$–$L_B$ plane, as in Fig. 4. The region that satisfies Eqs. (7) and (8) is shaded. Within this stability region we choose lengths $L_A = 6.9$ m and $L_B = 28.1$ m for each guideway segment. With these particular configuration lengths, the system is stable for the velocity range of 122 to 165 m/s. In general, a larger stability region, which occurs for larger values of $\alpha_1/\beta_1$ and $\beta_2/\alpha_2$, implies a larger velocity range for which the system is stable.

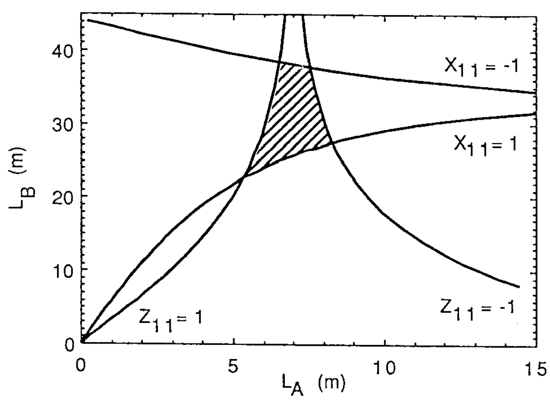


Fig. 4. Stability plot for v = 139 m/s, $\alpha_1 = 42.2$ m$^{-1}$, $\alpha_2 = 13.4$ m$^{-1}$, $\beta_1 = 58.2$ m$^{-1}$, $\beta_2 = 10.0$ m$^{-1}$. The shaded region indicates choices of guideway segment lengths $L_A$ and $L_B$ for which the system is dynamically stable.

The rail geometry is an important design concern. For example, if the rails in each configuration in the above example had a 50 mm by 50 mm cross section and were placed so that $D_A > D_C = D_B$, the gradient coefficients would be $\alpha_1 = 25.0$ m$^{-1}$, $\alpha_2 = 17.7$ m$^{-1}$, $\beta_1 = 71.9$ m$^{-1}$, $\beta_2 = 7.2$ m$^{-1}$. The resulting velocity range for stability would be 136 to 143 m/s.

The static-field solution is useful only if the magnetic diffusion time is short compared to the residence time of the vehicle magnet over the iron. The magnetic diffusion time is defined by

$$\tau = \mu \sigma d^2 / \pi^2, \tag{9}$$

where $\mu$ is the permeability, $\sigma$ is the electrical conductivity, and d is the thickness of the medium. In the levitation example, much of the iron is saturated with $\mu$ of order 2. With $\sigma = 1.7\times10^6$ siemens/m and d = 20 mm, $\tau$ = 0.09 ms. This value is considerably less than the 10-ms residence time of a 1.4-m-long magnet over a position on the rail at a vehicular speed of 140 m/s. For the example geometries described above, the transient solver of PE2D [9] was used to solve for the magnetic field as a function of time when a step-function boundary condition was used for the current in the vehicle coils. In all cases, the calculated magnetic force increased to over 95% of the static-solution value in less than 1 ms.

The magnetic drag resulting from eddy currents in the iron rails could be kept to a minimum by conventional lamination or possibly by the use of sintered iron.

### Vehicular Trajectory

Stability calculations for an actual HSGT system must account for all degrees of freedom in three dimensions, and include the forces of aerodynamics and propulsion as well as those of gravity and magnetic levitation. However, insight into the influence of the nonlinearities inherent in an iron-based attractive system can be gained by examining the simplified two-dimensional system. Equations (5)-(8) are strictly valid only for constant gradient coefficients, but within the region of stability, the system is stable to any amount of perturbation. As seen in Fig. 2, the forces in the vertical direction are nonlinear with z, and, in addition, there is some variation of the vertical force with displacement in the x direction. In general, the nonlinearities of the system decrease the region of stability.

Using the force curves generated by the static solver of PE2D and ignoring damping of motion and rotation about the y axis, we numerically integrate vehicular trajectories to determine the domain of stability for deviations in x, z, $v_x$, and $v_z$ about equilibrium. The results indicate that step-function perturbations of several mm and oscillations of up to 15 mm can be tolerated. Such results indicate that larger guideway imperfections are tolerable in this system, compared with an EMS system.

### System Considerations

The use of iron, combined with the large guideway clearance, should result in a lower cost track, especially if the iron can also be used as a structural support for suspended spans of guideway. The large guideway clearance reduces the required rigidity relative to EMS designs. On a volume basis, iron costs less than copper or aluminum, which must be used with the EDS method. The cross sectional area of 30 cm$^2$ for the guideway in the examples used in this paper compare favorably with the 160 cm$^2$ [10] and 140 cm$^2$ of several continuous-sheet EDS designs. In some geometries, the use of iron above the superconducting magnets helps to reduce the magnetic field strength within the passenger compartment.

The wide variety of rail materials and geometries that are available should enable a choice over a relatively large range of stiffness parameters in the magnetic suspension system. The region of stability could be improved further by using steel rails with oriented permeabilities. Smaller stiffness in the magnetic suspension is generally associated with a smaller region of stability in Configuration A. The guideway clearance can be increased, or the coil current decreased, by adding more iron to the guideway.

### Conclusions

The use of alternating-gradient attractive levitation offers the potential of a HSGT system with negligible magnetic drag and large guideway clearance without the need for active feedback for stability. The concept of alternating-gradient attractive levitation is still in the early stages of development for applications to HSGT. Only a few simple geometries have been analyzed for stability, and factors such as trade-off in ride quality versus degree of track imperfection have yet to be examined. To apply this concept to a realistic HSGT system will require considerably more invention.

### Acknowledgments

This work has been sponsored by the U.S. Department of Energy, Office of Transportation Research, under Contract W-31-108-ENG-38.

### References

1. J. R. Powell and G. T. Danby, "Magnetic Suspension for Levitated Tracked Vehicles," *Cryogenics*, **11**, 192-204, 1971.

2. G. T. Danby and J. R. Powell, "Design Approaches and Parameters for Magnetically Levitated Transport Systems," in *Superconductivity and Its Applications*, eds., H. S. Kwok and D. T. Shaw, Elsevier, New York, 1988, pp. 318-342.

3. G. M. Asher, J. T. Williams, R. J. A. Paul, and J. Brown, "Current Research into Mixed-Mu Levitator Designs for High Speed Maglev Vehicles," *J. de Phys.* **C1**, 733-738, 1984.

4. E. D. Courant and H. S. Snyder, "Theory of the Alternating Gradient Synchrotron," *Ann. Phys.*, **3**, 1-48, 1958.

5. J. J. Livingood, *Principles of Cyclic Particle Accelerators*, D. Van Nostrand, New York, 1961.

6. M. S. Livingston and J. P. Blewett, *Particle Accelerators*, McGraw-Hill, New York, 1962.

7. J. R. Hull, "Efficiency of Passive Magnetic-Confinement Methods for Rapidly Rotating Solid Rings," *J. Appl. Phys.*, **58** 3594-3600, 1985.

8. W. Braunbek, "Freely Suspended Bodies in Electric and Magnetic Fields," *Z. Phys.*, **112**, 753-763, 1939.

9. Vector Fields Ltd., 24 Bankside, Kidlington, Oxford OX5 1JE, England.

10. G. Slemon, "The Canadian MAGLEV Project," in *Transport Without Wheels*, ed., E. R. Laithwaite, Elek Science, London, 1977, pp. 74-88.

11. H. H. Kolm, R. D. Thornton, Y. Iwasa, and W. S. Brown, "The Magneplane System," *Cryogenics*, **15**, 377-384, 1975.